EVALUATION OF AN APPROXIMATE METHOD FOR INCORPORATING FLOATING DOCKS IN HARBOR WAVE PREDICTION MODELS

A Thesis

by

ZHAOXIANG TANG

Submitted to the Office of Graduate Studies of
Texas A&M University
in partial fulfillment of the requirements for the degree of

MASTER OF SCIENCE

August 2005

Major Subject: Ocean Engineering

EVALUATION OF AN APPROXIMATE METHOD FOR INCORPORATING

FLOATING DOCKS IN HARBOR WAVE PREDICTION MODELS

A Thesis

by

ZHAOXIANG TANG

Submitted to the Office of Graduate Studies of
Texas A&M University
in partial fulfillment of the requirements for the degree of

MASTER OF SCIENCE

Approved by:

Co-Chairs of Committee,	Billy L. Edge
	Vijay Panchang
Committee Members,	Prabir Daripa
	Tom Ravens
	Jun Jin
Head of Department,	David V. Rosowsky

August 2005

Major Subject: Ocean Engineering

ABSTRACT

Evaluation of an Approximate Method for Incorporating Floating

Docks in Harbor Wave Prediction Models. (August 2005)

Zhaoxiang Tang, B.E., Harbin Engineering University

Co-Chairs of Advisory Committee: Dr. Billy L. Edge
Dr. Vijay Panchang

Computer models are nowadays routinely used in harbor engineering applications. Models based on the two-dimensional elliptic mild-slope equation can simultaneously simulate refraction, diffraction, reflection, and dissipation in completely arbitrary coastal domains. However, floating structures such as floating breakwaters and docks are often encountered in the modeling domain. This makes the problem locally 3-dimensional. Hence it is problematic to incorporate a floating structure into the 2-d model. Tsay and Liu (1983) proposed a highly simplified but approximate approach to handle this problem practically. The validity of their approach is examined in detail and it is found that the actual solutions deviate considerably from the theoretical solutions, although their approximation provides results with the correct trend. Therefore, correction factors have been developed and may be used to produce more reliable results using the framework of Tsay and Liu (1983). The resulting method is applied to Douglas harbor in Alaska. The result shows that docks in the harbor distort the wave field considerably and create a reflective pattern that can affect navigation safety in some areas. Also plots are developed for the transmission coefficients for waves propagating

past rectangular and cylindrical floating objects of infinite extent for a wide range of conditions encountered in practice.

ACKNOWLEDGMENTS

I wish to express my deepest appreciation to Professor Vijay Panchang for his valuable instructions and encouragement throughout this work, and my special thanks to Mr. Dongcheng Li for his valuable suggestions during this work.

I also appreciate the valuable instruction and the constructive criticism received from Prof. Billy L. Edge, Prof. Prabir Daripa, Prof. Jun Jin, and Prof. Tom Ravens during my study.

Finally special thanks are given to Dr. Zeki Demirbilek of the US Army Corps of Engineers for technical advice during this work.

TABLE OF CONTENTS

LIST OF FIGURES

FIGURE Page

CHAPTER I

INTRODUCTION

Motivation

The past several years have seen the development of sophisticated coastal wave transformation models, which can simultaneously simulate refraction, diffraction, reflection, and dissipation in completely arbitrary coastal domains (for example, the model CGWAVE, Demirbilek and Panchang 1998). Based on different mathematical formulations, these models are mainly categorized as two types of models: phase-resolving (or mass-balance) models and phase-average (or energy-balance) models. Phase-resolving models are based on a mass-balance formulation, while phase average models such as SWAN (Booij et al. 1999; Ris et al. 1999) are based on the energy-balance equation. Phase-average wave models are suited to large scale wave growth and wave transformation applications, while phase-resolving wave models are better suited to domains with complex bathymetric and geometric features where the effects of wave diffraction and reflection can be important. Phase resolving models are based on the elliptic mild or steep slope equation (e.g., Berkhoff 1972; Chamberlain and Porter 1995), which is applicable to the full spectrum of water waves, or on the Boussinesq equations (e.g., Madsen and Sorensen 1992; Nwogu 1993; Wei et al. 1995), which are traditionally limited to shallow water waves.

In projects involving harbor/marina design or modifications, computational models based on the elliptic mild-slope wave equation are often used to calculate the

---

This thesis follows the style and format of Coastal Engineering.

requisite wave properties, including the effects of wave refraction, diffraction, and reflections in regions with arbitrary geometry. In recent years, development of several codes to solve this equation and of sophisticated finite-element grid generators and graphical user interfaces has resulted in many practical models. Well-known models used by engineers include PHAROS, CGWAVE, and EMS. They have been used in studies of Ste. Therese de Gaspe Harbor, Kahului Harbor, Morro Bay Harbor, Venice Lagoon, Los Angeles/Long Beach Harbor, Barbers Point Harbor, etc. (Tang et al. 1999; Thompson and Demirbilek 2002; Thompson et al. 2002; Panchang and Demirbilek 2001; Mattioli 1996; Kostense et al. 1988; Bova et al 2000; Zubier et al. 2003; and others).

When applying models based on mild-slope models to actual harbor/marina projects, engineers often meet with the situation, where floating structures exist in the modeling domain (e.g., floating breakwaters or docks in marinas). These structures violate the equation's "free-surface" requirement. Although full three-dimensional models are available (e.g., Yue et al. 1976), these models assume a flat ocean bottom of infinite extent. No models are available at present for solving the full 3-d problem for a typical harbor with all its coastal boundary and depth variations.

Mathematical Background

The governing equation for mild-slope wave models is:

$$\nabla \,.\, (CC_g \, \nabla \Phi) + (k^2 CC_g)\Phi \;=\; 0 \tag{1}$$

In equation (1), $\Phi(x,y)$ is the complex wave velocity potential, C is the wave velocity, C_g is the group velocity, and k is the wave number. (The last three quantities are determined on the basis of the local depth $h(x, y)$ and the given wave frequency.) The wave height and phase may be estimated from Φ. Equation (1) is a two-dimensional, vertically-integrated form of the time-harmonic complex Laplace equation

$$\nabla^2 \phi(x,y,z) = 0 \tag{2}$$

where

$$\phi(x,y,z) = f(\mathrm{z})\, \Phi(x,y) \text{ and } f(z) = (\cosh k(z+h))/\cosh(kh). \tag{3}$$

The vertically integrated form (1), together with the assumption (3), has been demonstrated to be valid for $|\nabla h|/kh << 1$ (Berkhoff 1976). This criterion is usually met in most applications. The elliptic equation (1) represents a boundary-value problem, and can have internal depth variations and boundaries. It is therefore widely used for performing wave simulations in regions with arbitrarily-shaped (manmade or natural) boundaries and arbitrary depth variations. Unlike the parabolic approximation (e.g., Panchang et al. 2000) which has limitations on the angle of wave incidence or the degree and direction of wave reflection and scattering that can be modeled, equation (1) is more general.

In this thesis, two methods are explored to solve the elliptic mild-slope equation, simultaneously addressing the effects of confined regions with variable bathymetric and geometric features and a floating structure. The first method (Method 1) examined coupling a 3-d model based on equation (2) in the vicinity of the structure with a 2-d model, based on the vertically averaged equation (1) in the surrounding area.

Difficulties in the use of this method would be addressed. The second method (Method 2) examines an approximate but simpler alternative procedure that is based on a strategy first proposed by Tsay and Liu (1983). This approach does not violate the overall two-dimensionality of the problem. The validity of their approach is examined in detail and it is found that although their approximation provides results with the correct trend, the actual solutions deviate considerably from the theoretical solutions. Therefore correction factors have been developed and may be used to produce more reliable results using the framework of Tsay and Liu (1983).

Method 1

This involves interfacing a locally 3-d model (near the floating structure) with a 2-d model in the rest of the harbor domain. Solving the fully 3-dimensional (2) over the whole domain is computationally prohibitive. Therefore the approach of constructing two models in the whole domain was examined by Panchang (2005): one is based on the 3-d equation (2) and applies only in the immediate vicinity of the structure (Figure1); elsewhere another model based on the 2-dimensional (1) is applicable. The two models could then be coupled at the interface.

In the shaded area (Figure1), the boundary element method was used by Panchang (2005) to solve the 3-d model, which involved placing grids only on the boundaries. The "curtain" and the structure itself were discretized into "panels". The panels used were triangular, and the 3-dimensional problem was solved following the boundary element method for most floating structures (e.g. Sarpkaya and Isaacson, 1981).

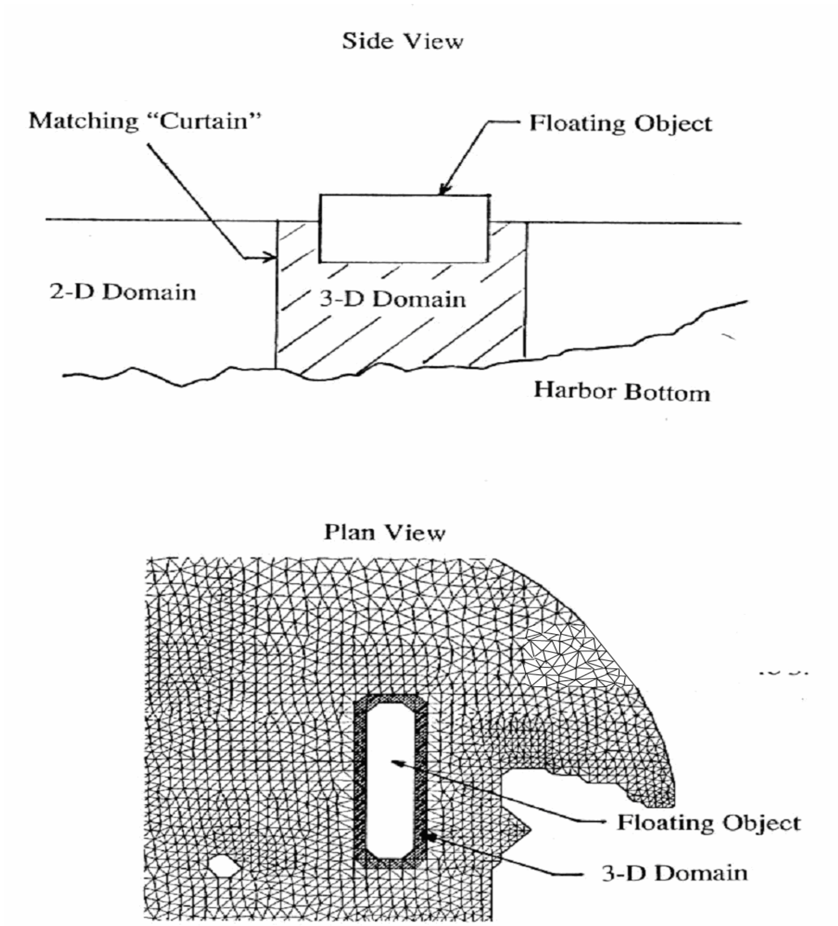

Figure 1. 2-D and 3-D model domains.

Elsewhere, the 2-d model was solved by the finite element method. The linear equation system was solved by conjugate-gradient method (Panchang et al. 1991). For matching along the interface, the solution and the derivative were both not known at the interface. So a guess was made, and based on the guess, ϕ or $\partial\phi/\partial n$ was used to force the next iteration.

Although the two models (the 2-d finite-element and the 3-d boundary element model) worked independently without difficulty, the iterative method for coupling the two solutions at the interface did not converge. Panchang (2005) made several attempts in order to achieve convergence, including changing the initial guess and switching the order of the coupling (i.e. normal derivative provided to the 3d model, solution provided to the 2d model), etc. But the problem of convergence was not solved. Recently, Koutandos et al. (2004) have gotten some success with this method, but their work was limited to the x-z plane only. Ohyama and Tsuchida (1997) also developed a 2d-3d model. The 2-d sub-domain has a hyperbolic vertical variation (as in (3)), the vertical variation in the 3-d sub-domain is described with a series of cosine functions. But their method is too difficult to apply for real-world application.

Method 2

In view of the difficulties of the rigorous approach, in this thesis an approximate method suggested by Tsay & Liu (1983) for tackling floating structures in the context of 2-d harbor wave models was explored in detail. This approach, referred as the TL-approximation for convenience, merely calls for suppressing the second term on the left-hand side of (1). As a consequence, the method is extremely simple to implement with existing finite element models. A model grid is first generated as usual without presence of the floating structure, grid elements covering the floating structure (in plan view) are selected, they are assigned a depth value equal to the under-keel clearance, and the coefficient of the second term in (1) is set to zero for these elements. Clearly, this is an approximate method intended for convenience in engineering practice. Tsay and Liu (1983) justified their approach on the grounds that under the structure, the basic continuity equation holds, while outside the area of the structure, the wave equation (2) holds. In reality, wave motion exists under the structure also. Although Tsay & Liu (1983) provided such arguments in support of this approach, their testing of this procedure was rather limited.

Project Goals

In view of the potential efficiency of this approach (relative to the full 3-d solution), a detailed examination of the limits of this approximation was undertaken, with the goal of determining the errors for a wide spectrum of commonly encountered parameters. The parameters are the relative width *ka* and the relative submergence *d/h* (where *a* = characteristic structure size, *d* = draft). This investigation is done by comparing the full Laplace equation with the TL-approximation. The mathematical formulation and solution method are given in Chapter II. Through numerical experiments, attempts have been made to develop modifications to the TL-approximation that can minimize its errors (Chapter III), thus improving the performance of this approximation for practical problems. In Chapter IV, the modified TL-approximation is validated using three independent tests for which theoretical solutions and/or data are available. A byproduct of this thesis consists of plots of transmission coefficients for waves passing an infinitely long cylinder and a rectangular floating structure. These problems have been solved analytically (to some extent) in the past. But complex code must be developed to actually calculate these coefficients. In fact, the US Army Corps of Engineers' Coastal Engineering Manual (referred to as CEM) provides these coefficients only for a specific geometry as regards a rectangular floating breakwater, and Martin and Dixon (1983) provide these values only for a specific cylinder geometry in deep water. Plots for the entire range of *kh*, *ka*, and *d/h* values likely to be encountered in practice are provided. In Chapter V, a demonstration of the use of the proposed method is provided, along with a 2-dimensional finite-element wave model, in Douglas Harbor (Alaska). The effects of incorporating the floating docks in the model are quite distinct and show that the presence of the docks can create strong reflections which could adversely impact small-craft operation in some areas.

CHAPTER II

THE FINITE DIFFERENCE FORMULATION

Numerical experiments are performed to compare the solutions of the full Laplace equation to the TL-approximation. For this purpose, the case of a rectangular floating object of infinite extent is used. The problem shown in Figure 2 is solved. Based on the difference between the above 2 solutions, the correction factors would be developed to make the solution of TL-approximation match the theoretical ones. In this chapter, the finite difference methods are described to get the theoretical solution for the 2-D Laplace equation for a wave propagating past one floating dock, and also to obtain a solution for the 1-D TL-approximation. Based on the difference between the above 2 solutions, correction factors can be developed to make TL-approximation solution match with theoretical solutions.

Mathematical Formulation for the Laplace Equation

The problem is to estimate the transmission and reflection coefficients associated with the propagation of a monochromatic wave on a flat sea bed past an infinitely long, fixed, floating structure of rectangular cross-section (Figure 2).

An incident wave $\phi_i = (H_i/2)\ exp(ikx)\ f(z)$ is specified at the left boundary HA. (Here, the incident wave height H_i is set as 2 meter). The left and right boundaries are placed far enough away from the structure so that the vertical distribution for the components propagating away from the structure may be assumed to be $f(z)$. Along the left boundary HA, the combination of the incident wave and an unknown reflected wave of the form $\phi_r = (H_i/2)\, Rexp(-i(kx+\beta)\, f(z)$ (where R is the reflection coefficient and β is the phase shift on the upwave side) gives rise to the following boundary condition (Panchang et al. 1991):

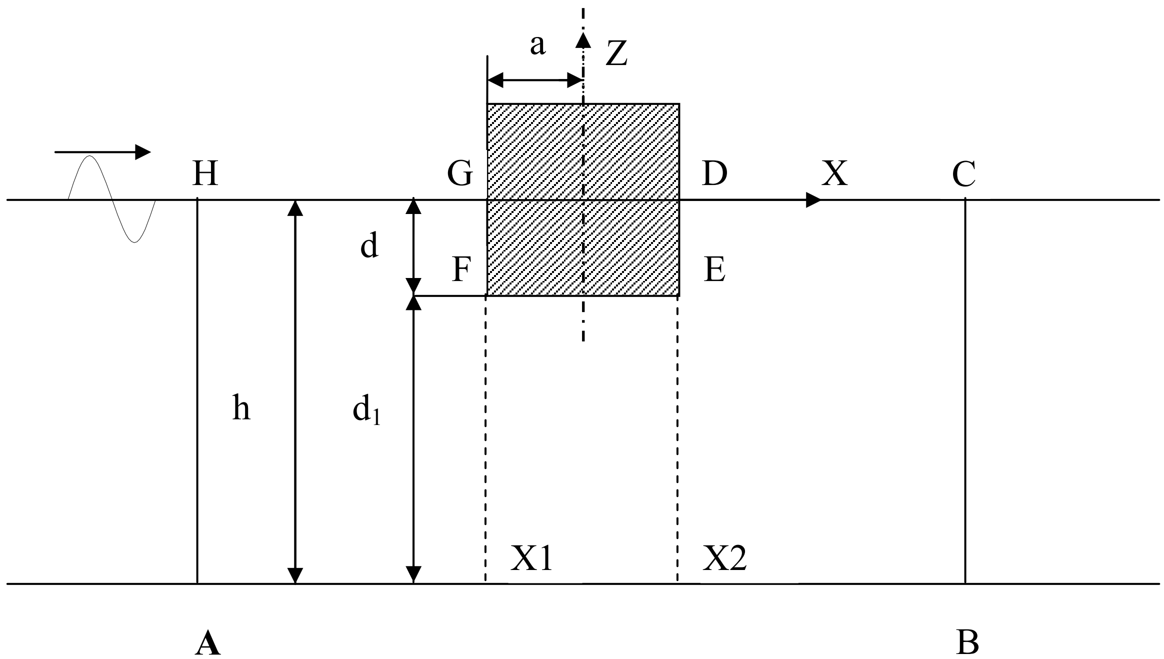

Figure 2. Wave transmission past a rectangular floating structure of infinite extent.

$$\partial\phi/\partial x = ik(2\, f(z) - \phi) \tag{4}$$

Along the right boundary CB, the boundary condition associated with an unknown transmitted wave (of the form $Texp(i(kx + \delta))\, f(z)$) may be written as

$$\partial\phi/\partial x = ik\phi \tag{5}$$

where T is the amplitude of the transmitted wave and δ is the phase shift.

Along the free surface HG and DC, the boundary condition is:

$$\partial\phi/\partial x = (\sigma^2/g)\phi \tag{6}$$

And, finally, along the seabed AB and the boundaries of the structure GF, FE, and DE, the normal derivative is set equal to zero.

Solution by the Finite Difference Method

The finite difference scheme (as shown in Figure 3) is used to discretize the 2-dimensional Laplace equation ($\nabla^2 \phi\ (x,z) = 0$) and all of its boundary conditions, including the (4), (5), (6), and others. For convenience, the structure is placed the half way along the horizontal domain length.

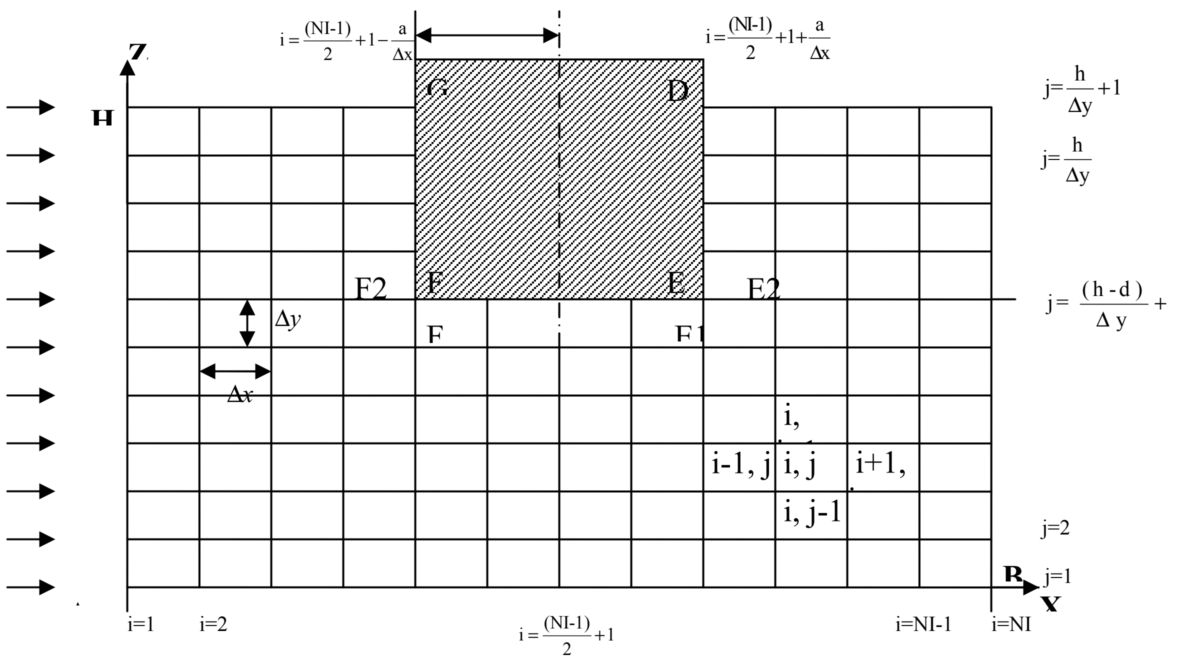

Figure 3. Finite difference scheme.

After discretization, the governing equation $\nabla^2 \phi\,(x,z) = 0$ becomes

$$\phi_{i-1,j}\Delta y^2+\phi_{i,j-1}\Delta x^2+(-2\Delta y^2-2\Delta x^2)\phi_{i,j}+\phi_{i,j+1}\Delta x^2+\phi_{i+1,j}\Delta y^2=0 \tag{7}$$

Here the central difference scheme is used.

The left boundary condition along AH, represented by equation (5), is discretized as:

$$(-2+\Delta xik)\phi_{1,j}+(2+\Delta xik)\phi_{2,j}=4\Delta xik\frac{\cosh k(h+z)}{\cosh kh} \tag{8}$$

The bottom boundary condition along AB, represented by equation $\frac{\partial\phi}{\partial z}=0$, becomes

$$\phi_{i,2}=\phi_{i,1} \tag{9}$$

The right boundary condition along BC, represented by equation (6), is discretized as:

$$\phi_{NI-1,j}(-2-\Delta xik)+\phi_{NI,j}(2-\Delta xik)=0 \tag{10}$$

The surface boundary condition along CD and GH, represented by equation (7), is discretized as:

$$\phi_{i,\frac{h}{\Delta y}+1}(2-\frac{\omega^2}{g}\Delta y)+\phi_{i,\frac{h}{\Delta y}}(-2-\frac{\omega^2}{g}\Delta y)=0 \tag{11}$$

On the structure's right side, the boundary condition along DE is discretized as:

$$\phi_{\frac{(\mathrm{NI}-1)}{2}+1+\frac{\mathrm{a}}{\Delta \mathrm{x}},j}=\phi_{\frac{(\mathrm{NI}-1)}{2}+2+\frac{\mathrm{a}}{\Delta \mathrm{x}},j} \tag{12}$$

Along the structure's bottom, the boundary condition along EF is discretized as:

$$\phi_{i,\frac{(\mathrm{h}-\mathrm{d})}{\Delta \mathrm{y}}+1}=\phi_{i,\frac{(\mathrm{h}-\mathrm{d})}{\Delta \mathrm{y}}} \tag{13}$$

On the structure's left side, the boundary condition along FG is discretized as:

$$\phi_{\frac{(\mathrm{NI}-1)}{2}+1-\frac{\mathrm{a}}{\Delta \mathrm{x}},j}=\phi_{\frac{(\mathrm{NI}-1)}{2}-\frac{\mathrm{a}}{\Delta \mathrm{x}},j} \tag{14}$$

Finally the resulting system of equations may be expressed in matrix form as

$$[A]\{\phi\}=\{f\} \tag{15}$$

where $[A]$ is the system matrix, $\{\phi\}$ is the unknown vector (of the desired grid-point values of the wave potential), and $\{f\}$ is a vector that contains information from the discretized boundary conditions. One method to solve the above equation group is

Gaussian elimination, which requires storage for the matrix $[A]$. Note that even when there are as few as 100 unknowns, $[A]$ contains 100*100 complex elements. Therefore computer storage can be one problem, and solution by direct Gaussian elimination is practically impossible for big domains. (In this study, the domain contains at least 7 wave lengths.)

As an alternative to Gaussian elimination, the resulting discretized system of linear equations is solved by the method of conjugate gradients (Panchang et al. 1991). The domains used here were typically at least 7 wavelengths long and at least 17 layers in the vertical. Also $\Delta x = \Delta z$ is used, thus ensuring a very high level of resolution and accuracy in the solutions. The following section presents the detailed procedure.

Solution by Iteration

The resulting discretized system of linear equations can be solved by the method of conjugate gradients (Panchang et al. 1991). This method does not require the storage of $[A]$, but it converges only when the system matrix is symmetric and positive-definite. In order to use the conjugate gradient method, the matrix $[A]$ must to be modified to be symmetric and positive-definite, or else the conjugate gradient method will not converge.

The existence of corner points, including A, B, C, H, F, E, D and G, destroys the symmetry of matrix $[A]$. Therefore the following procedures are followed to calculate the solution in the whole domain: first all above-mentioned corner points are removed from the original calculation domain and the conjugate gradient method can be used to acquire the values of the remaining nodes if the remaining calculation domain is symmetric. Then the values of unknown corner points would be acquired based on known values of nodes through related boundary conditions. However, it is found that even when the corner points are removed the remaining part of calculation domain is still not symmetric, since nodes E1 and E2 separately are related with the corner point E through equation (7); while similarly nodes F1 and F2 are separately related with the corner node F. Through analysis of boundary condition along DE, EF, and FG, it is found that the values at E, E1, and E2 equal each other, and similarly the values at F, F1, and F2 are identical as well. Based on this, the equation for E1 will become symmetric when replacing corner point E with the node E2, and that for E2 will become symmetric when replacing E with E1. Similarly the equations for nodes F1 and F2 can become symmetric as well. So through the above manipulation, the remaining part of domain is symmetric.

Although the system matrix $[A]$ is symmetric, it is still not positive-definite, and the basic conjugate gradient method will not work without some remedy. A remedy (Panchang et al. 1991) is to use the Gauss transformation, i.e. multiply equation (15) by $[A^*]$, the complex conjugate transpose of $[A]$:

$$[A^*][A]\{\phi\} = [A^*]\{f\} \tag{16}$$

The new coefficient matrix $[A^*][A]$ is always symmetric and positive-definite, and the modified CG procedure for equation [17] will converge. The algorithm is as follows:

1. Select trial values ϕ_0 (i.e. i=0^{th} iteration) for all grid points where the solution is desired.

2. Compute for all points $r_0 = f - A\phi_0$ and $p_0 = A^* r_0$.

3. Compute for i^{th} iteration: $\alpha_i = \dfrac{|A^* r_i|^2}{|Ap_i|^2}$

4. Update $\phi_{i+1} = \phi_i + \alpha_i p_i$.

5. Check for convergence of solution.

6. Compute, for each grid point, $r_{i+1} = r_i - \alpha_i A p_i$.

7. Compute for i^{th} iteration: $\beta_i = \dfrac{|A^* r_{i+1}|^2}{|A^* r_i|^2}$.

8. Compute $p_{i+1} = A^* r_{i+1} + \beta_i p_i$.

9. Set i=i+1, and go to step 3.

The above procedure is guaranteed convergence although the speed is slow. This is due to the coefficient matrix $\left[A^*\right]\left[A\right]$ of the transformed equation (16) having a far wider spectral range than the original matrix $\left[A\right]$.

Validation of the Code

The code for solving the Laplace equation was checked by comparing its results against the analytical solution presented by Drimer et al. (1992) for one case, for which 2*a/h*=2, *d/h*=0.7. In the code the water depth *h* is set as 4 m, characteristic structure size *a* as 4 m, and draft of floating structure *d* as 2.8 m. The solutions are practically indistinguishable from those in Figure 2 of their paper. (as shown in Figure 4)

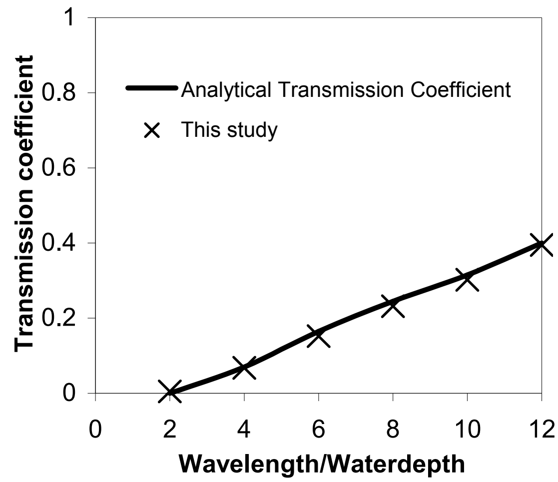

Figure 4. Comparison of analytical solution with code solution.

Solution of the TL-approximation

To obtain a solution for the TL-approximation, the governing equation (1) is rewrite as:

$$\partial(p\partial\Phi/\partial x)/\partial x + q\Phi = 0 \tag{17}$$

Φ for TL-approximation is different from that for Laplace equation.

where $p(x) = CC_g$ for all x; $q(x) = k^2CC_g$ for $x < x_1$ and $x > x_2$ and $q(x) = 0$ for $x_1 < x < x_2$. The extent of the structure is $x_1 < x < x_2$ (Figure 3). Note that to determine $p(x)$ when $x_1 < x < x_2$, Tsay and Liu (1983) recommend using the under-keel depth $d_l = h - d$.

While solving (17), the left boundary condition (4) (at x=0):

$$\partial\Phi/\partial x = ik(H_i - \Phi) \tag{18}$$

The right boundary (5) is valid here as well.

Based on finite difference method, after discretization, (17) becomes

$$p_1\Phi_{i-1} - (p_2 + p_1 - q_1\Delta x^2)\Phi_i + p_2\Phi_{i+1} = 0 \tag{19}$$

Here p_1, p_2, and q_1 are shown in Figure 5.

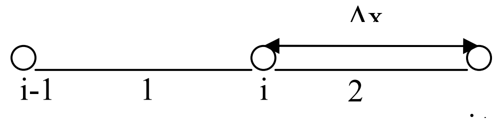

Figure 5. Central finite difference scheme for nodes.

Left boundary (4) becomes:

$$(\frac{\Delta x}{2} ik - 1)\Phi_1 + (\frac{\Delta x}{2} ik + 1)\Phi_2 = 2ik\Delta x \tag{20}$$

Similarly (5) becomes,

$$\Phi_N = (\frac{2 + ik\Delta x}{2 - ik\Delta x})\Phi_{N-1} \tag{21}$$

A solution to (17) may easily be obtained by the above finite-difference method, since discretization leads to a tridiagonal system of linear equations which can be easily solved by the Thomas algorithm.

CHAPTER III

COMPARISON OF THEORETICAL RESULTS WITH THE TL-APPROXIMATION

A total of 864 simulations was performed to cover a wide range of conditions encountered in practice ranging from shallow water to deep water, including kh = 0.1, 0.25, 0.4, 0.8, 1.2, 2, 2.8, 4, and 8. The size of the structure was described by $0 < ka < 5$ and its immersion by d/h = 0.25, 0.5, and 0.75 corresponding, respectively, to shallow, intermediate and deep draft.

In Figure 6 (a-i), all of the computed transmission coefficients are shown, including kh = 0.1, 0.25, 0.4, 0.8, 1.2, 2, 2.8, 4, 8 for d/h = 0.25, 0.5 and 0.75. The reflection coefficient can be computed based on $R^2 = 1 - T^2$. These curves may be used by engineers to supplement the single curve provided by the Coastal Engineering Manual (2001), which is applicable only for $0 < ka < 2.0$ and $d/h = 0.14$; or by Drimer et al. (1992), whose Figure 2 is applicable only for $a/h = 1$ and $d/h = 0.7$ in water of finite depth.

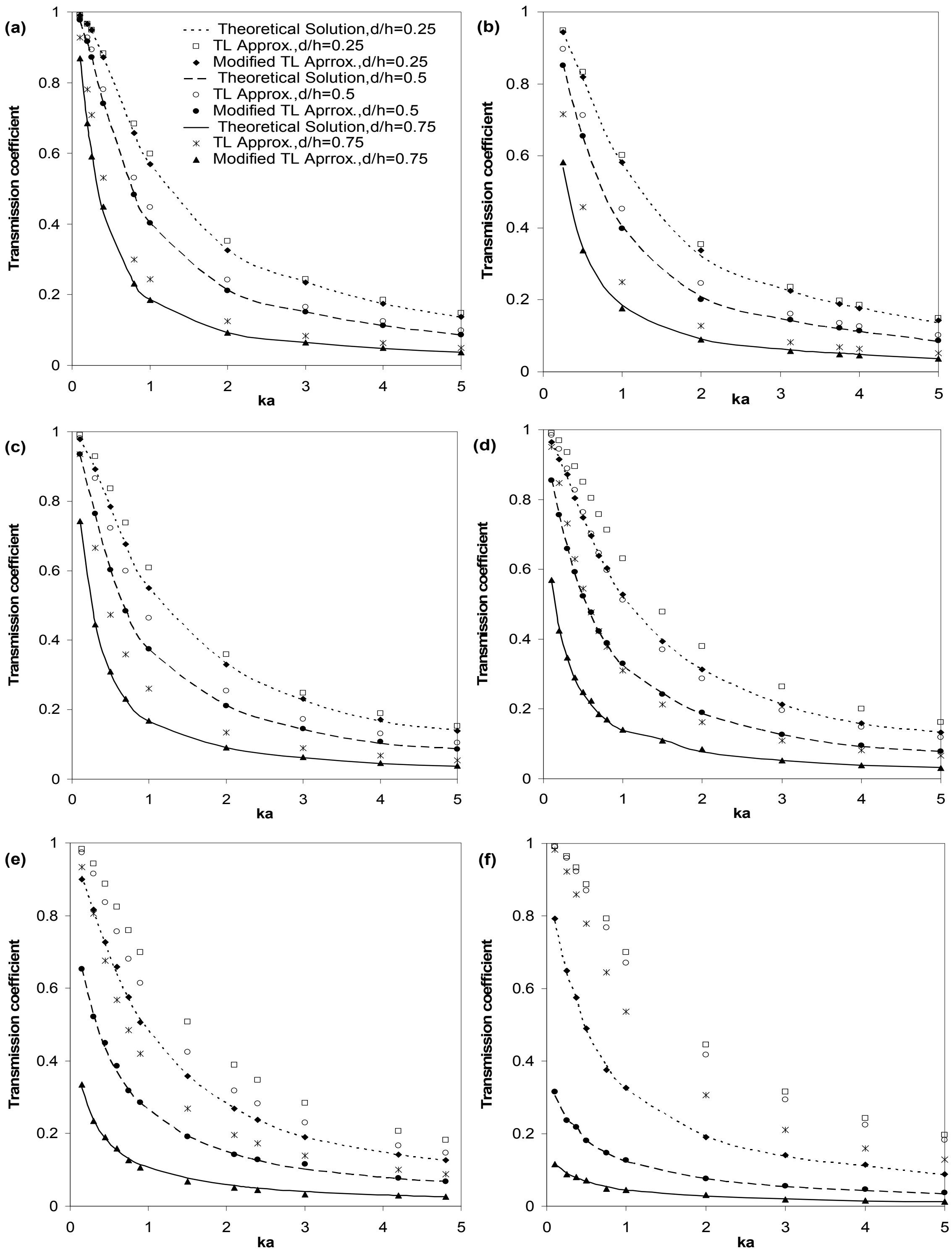

Figure 6. Modelled transmission coefficients for wave transmission past a rectangular floating structure of infinite extent. (a) kh=0.1, (b) kh=0.25, (c) kh=0.4, (d) kh=0.8, (e) kh=1.2, (f) kh=2.

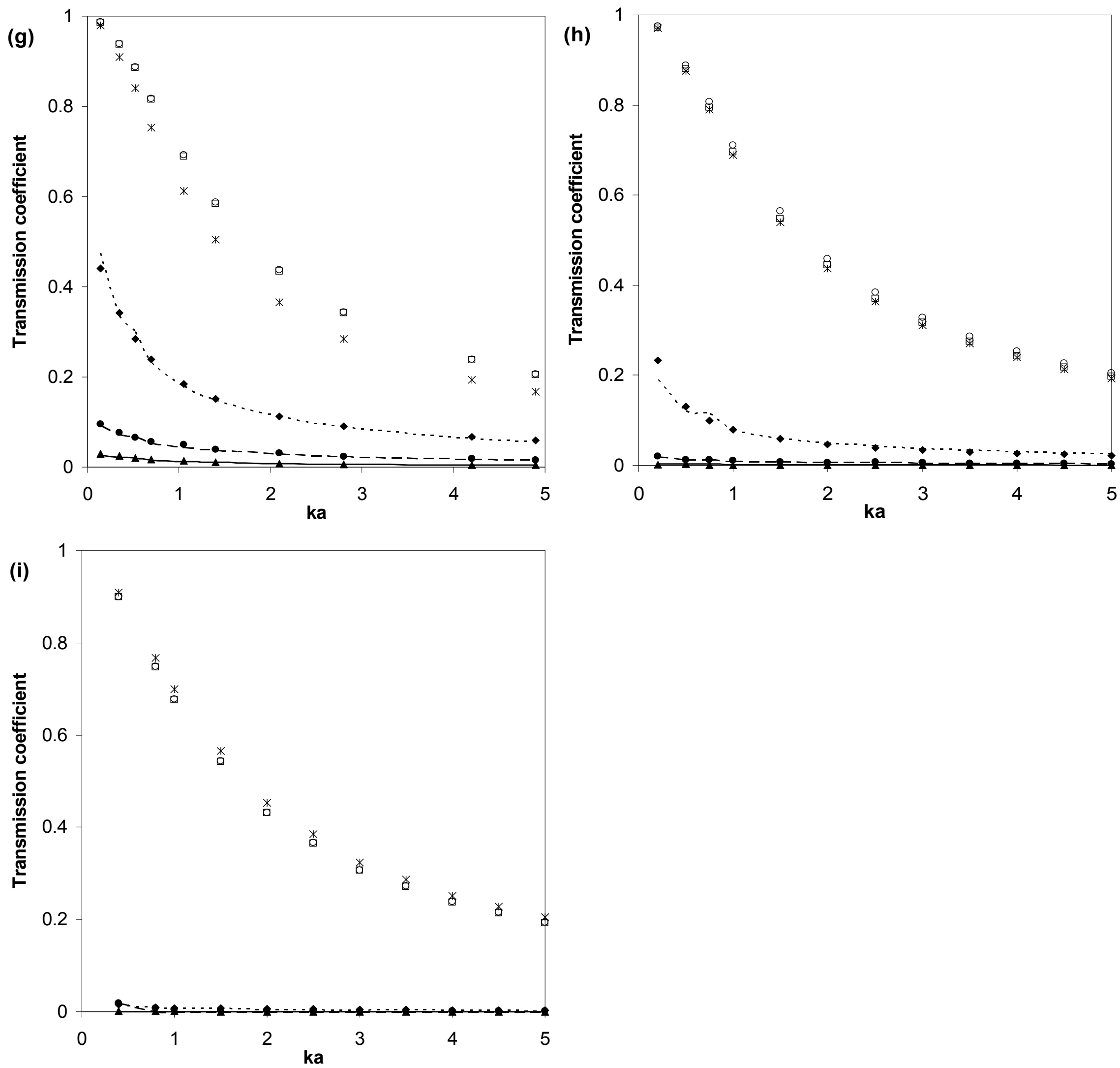

Figure 6. Continued. (g) kh=2.8, (h) kh=4, (i) kh=8.

The results of the TL-approximation are also plotted in Figure 6, and they appear to match the theoretical results very well in shallow water, but the degree of mismatch becomes high for intermediate and deep water. However, the TL-approximation shows the same trend as the theoretical solutions, and suggests that a simple ad-hoc adjustment to the method may yield results closer to the theoretical solutions. Among several possible ways of doing this, the approach of retaining q = 0 while adjusting p appropriately is examined (as per the original proposal of Tsay & Liu (1983)). While Tsay & Liu (1983) calculated p based on the under-keel clearance d_1, an attempt was made on a simple modification of the form αd_1, where α is a 'correction factor'. A large number of simulations were performed using trial values of α until the results of the "modified TL method" matched the theoretical solutions within 2%. The correction factors so obtained are shown in Figure 7.

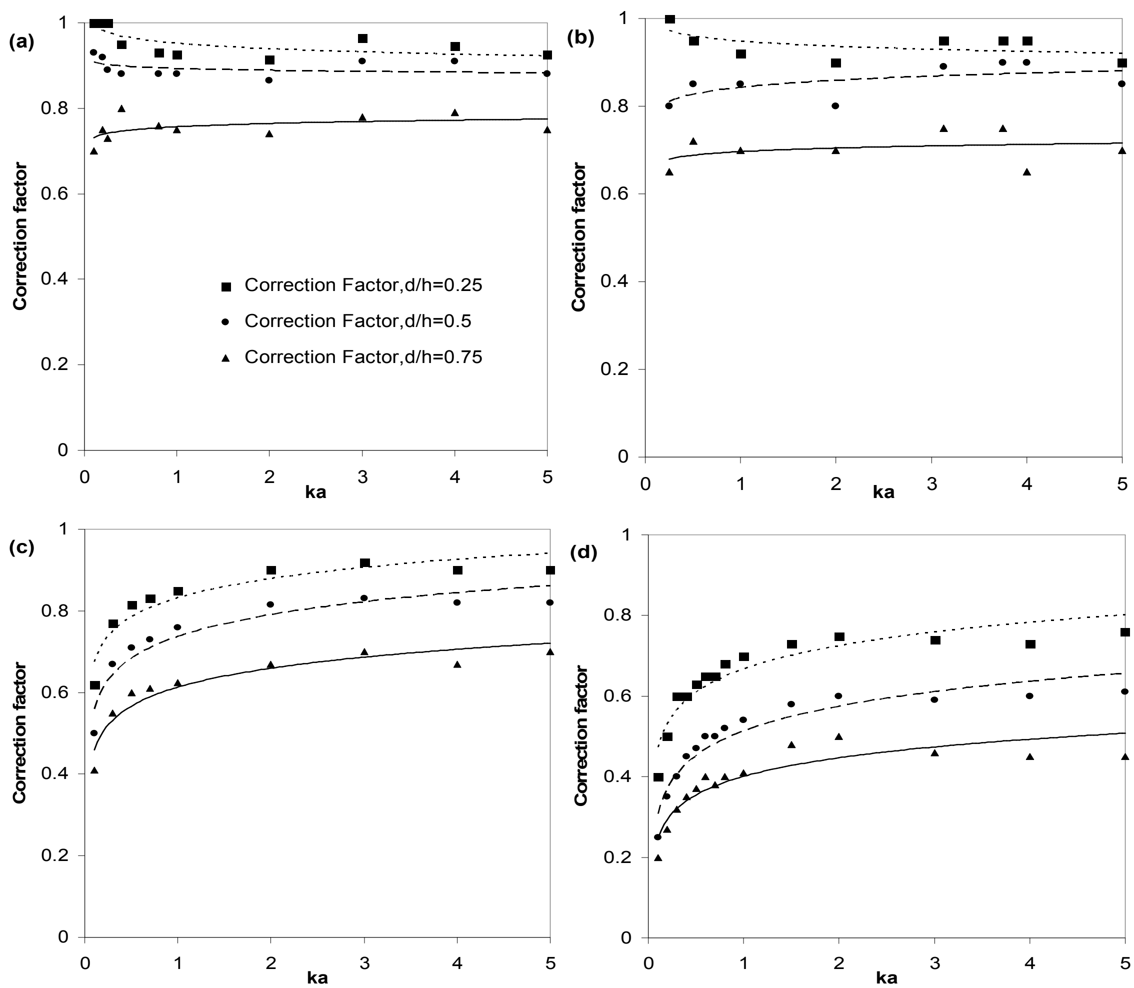

Figure 7. Correction factors and best-fit curves. (a) kh=0.1, (b) kh=0.25, (c) kh=0.4, (d) kh=0.8.

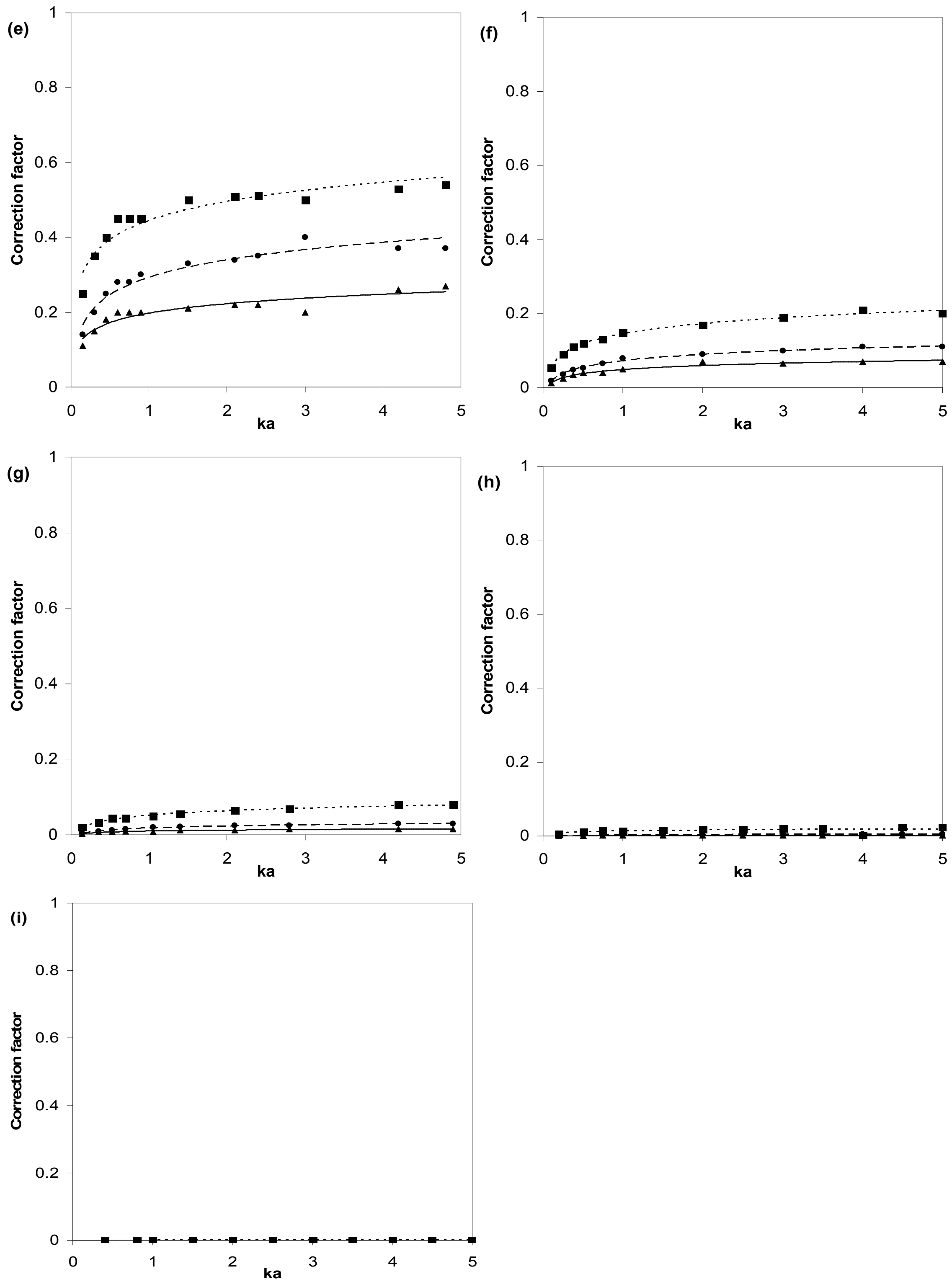

Figure 7. Continued. (e) kh=1.2, (f) kh=2, (g) kh=2.8, (h) kh=4, (i) kh=8.

For shallow water and shallow draft, α is roughly equal to unity (as expected). But for deep draft, the TL-approximation needs to be modified by $\alpha \approx 0.7$. For intermediate and deep water, α is not constant but shows an increasing trend with ka. In very deep water, the mismatch is large. Note that for short waves (relative to submergence), $T \to 0$. This requires us to create a high level of wave blockage, which can be accomplished by $\alpha \to 0$ with the modified TL-approximation, as seen in Figure 7 (for kh = 4). Of course this result would not hold if d/h were much smaller than the smallest value investigated here (which is typical in engineering practice).

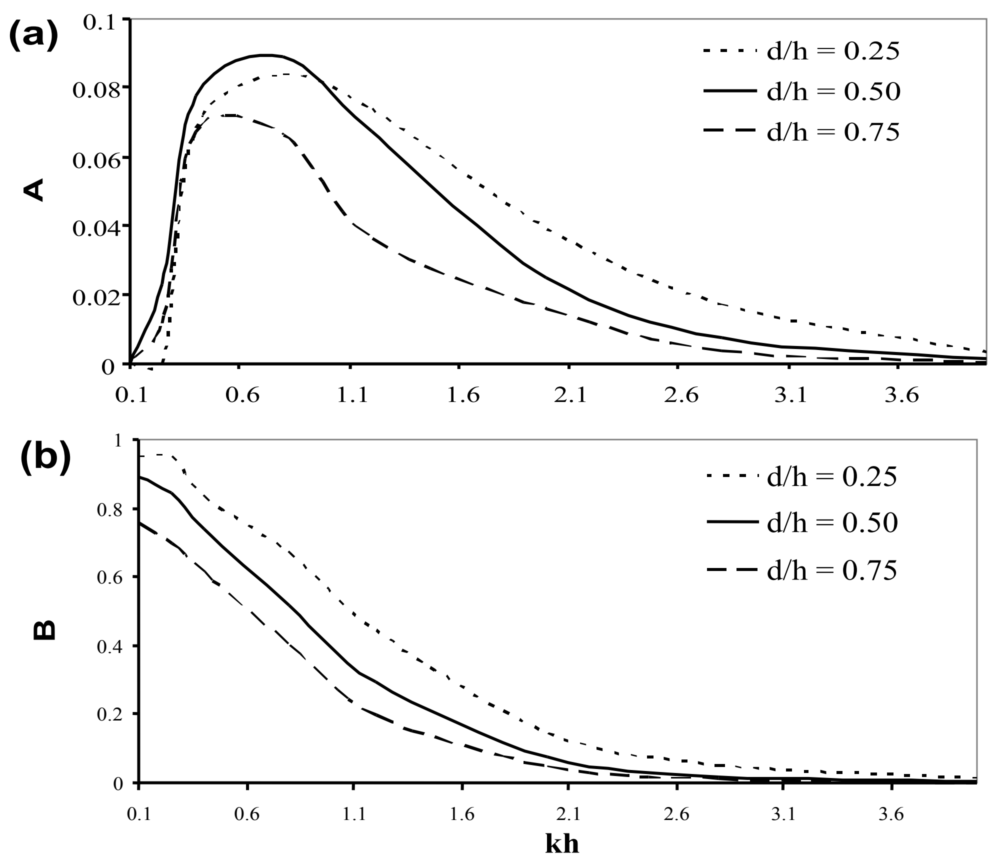

Figure 8. A and B values for determining α.

Plots similar to those in Figure 7 were produced for all cases examined. The best fit curve for these had the form of $\alpha = A ln(ka)+B$. The corresponding A and B are given in Figure 8. For $kh < 0.1$ and $kh > 4$, we recommend using the A and B values corresponding to these thresholds. For convenience, the numerical values corresponding to Figure 8 are given in Table 1.

TABLE 1. NUMERICAL VALUE CORRESPONDING TO FIG.7.

A

kh	0.1	0.25	0.4	0.8	1.2	2	2.8	4
$d/h = 0.25$	0	0	0.0681	0.0838	0.0737	0.0392	0.0173	0.0034
$d/h = 0.50$	0	0.0233	0.0776	0.0889	0.0675	0.0248	0.0074	0.0013
$d/h = 0.75$	0	0.0118	0.0669	0.0664	0.0364	0.0157	0.0036	0.0005

B

kh	0.1	0.25	0.4	0.8	1.2	2	2.8	4
$d/h = 0.25$	0.9525	0.9487	0.8321	0.6671	0.4454	0.1459	0.0522	0.0139
$d/h = 0.50$	0.8935	0.8431	0.7375	0.5138	0.2934	0.0731	0.0185	0.0028
$d/h = 0.75$	0.7568	0.6965	0.6133	0.401	0.1977	0.0491	0.0102	0.001

Results of the modified TL-approximation obtained with A and B values selected from Figure 8 are also plotted in Figure 6. As expected, the results are close to theoretical solutions.

CHAPTER IV

VALIDATION

In order to test the validity of the modifications proposed above for situations beyond the ones from which they were derived, the modified TL-approximation was applied to the following cases for which laboratory data or analytical solutions are available.

Square Floating Breakwater

Koutandos et al. (2004) have presented data pertaining to transmission coefficients for waves passing a fixed, infinitely long, floating breakwater of rectangular cross-section with d/h = 0.5 with a/h = 0.25. Although this case is similar to those described in Chapter II and III, the laboratory data can serve as an independent test of the modified TL-approximation. This case pertains to wave propagation in intermediate depths. The results of the original TL-approximation using the under-keel depth to calculate p are compared in Figure 9 with the lab data. It can be seen that there is considerable mismatch, which seems to be increasing with ka. On the other hand, the results of modified TL-approximation, obtained by using A and B values from Figure 8, show good agreement with the measured transmission coefficients.

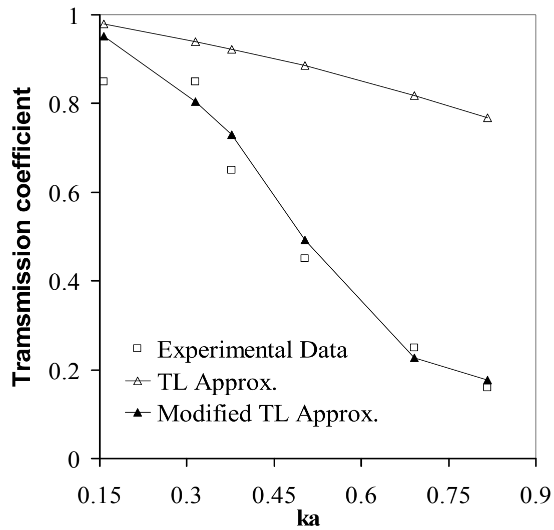

Figure 9. Wave height comparison with data presented in Koutandos et al. (2004).

Infinitely Long Cylinders

Ijima et al. (1976) calculated transmission coefficients for waves passing one infinitely long cylinder and two in-line cylinders (Figure 10) by solving the Laplace equation via the boundary element method. Their "theoretical" results, along with laboratory data they collected for these cases, are shown in Figure 11. These tests pertained to the intermediate water depth regime. While using the modified TL-approximation for these simulations, the under-keel clearance d_1 changes at every grid point. Although a variable α can be used, here an approximate value of α was estimated based on an equivalent rectangular immersed area of the same width as the cylinder. Figure 11 indicates that the results of the modified TL-approximation show much smaller discrepancies than those of original TL-approximation, when compared with both the theoretical results and the measured data provided by Ijima et al. (1976).

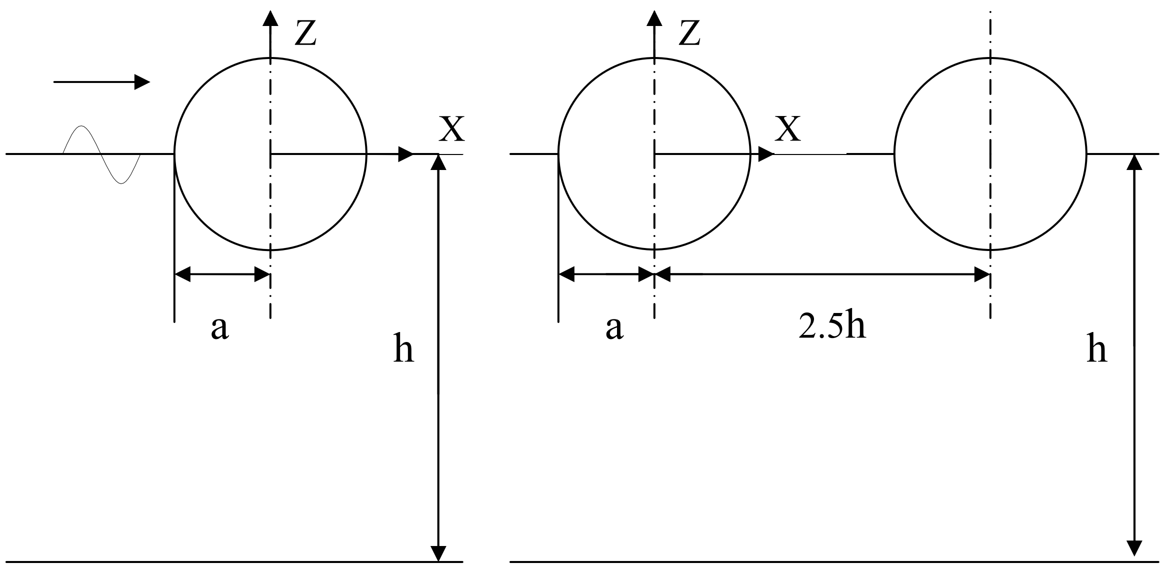

Figure 10. Wave transmission past floating cylinder(s) of infinite extent (a = 0.16m; h = 0.4 m).

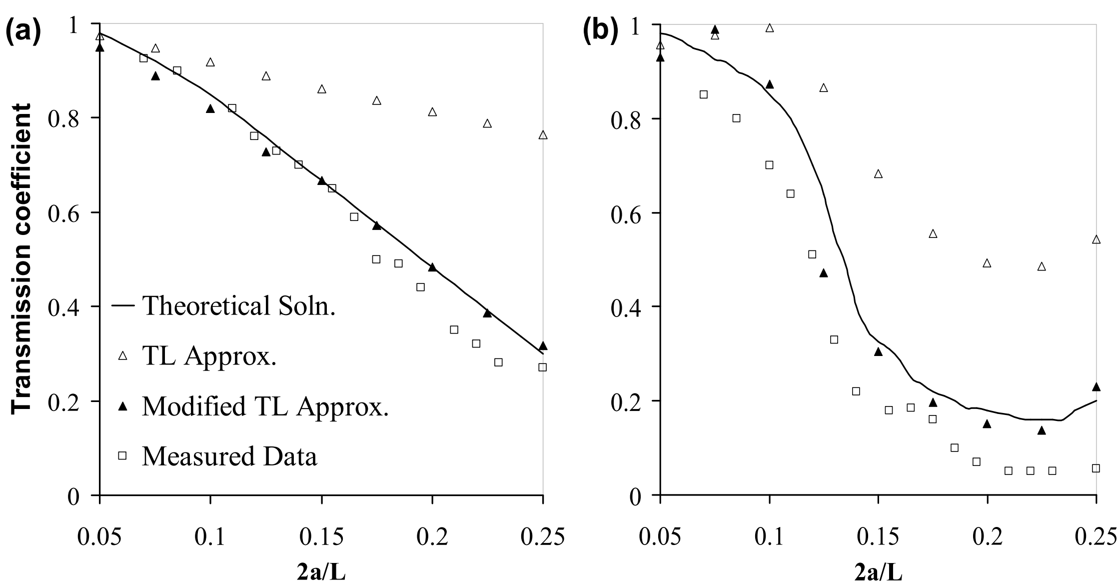

Figure 11. Wave height comparison. Theoretical solutions and data from Ijima et al. (1976). (a) one cylinder, (b) two cylinders.

For the case of similar cylinders in deep water, Martin and Dixon (1983) developed an analytical method to calculate the transmission coefficient and presented them in the form of a table for the practitioner's benefit. By way of validation, we performed numerical simulations in the deep water regime for *ka* > 3. (Smaller values of *ka* lead to smaller values of *d/h* ratios for a cylinder with its centerline corresponding to the water surface, as in Figure 10). The results, shown in Figure 12, again indicate that the modified TL-approximation is a significant improvement compared with the original approximation.

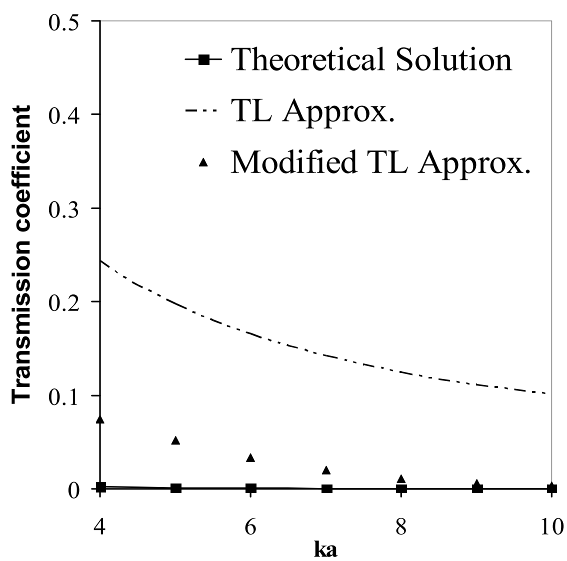

Figure 12. Wave transmission coefficients for wave propagation past a cylinder in deep water.

Since these simulations of selected cases pertaining to infinitely long cylinders show that the modified TL-approximation is able to reproduce the theoretical results reasonably well, used as a surrogate for the Laplace equation, curves were developed for transmission coefficients in shallow, intermediate and deep water depth. These curves, provided in Figure 13, may be used by the engineer to supplement the table provided by Martin and Dixon (1983) for deep water applications.

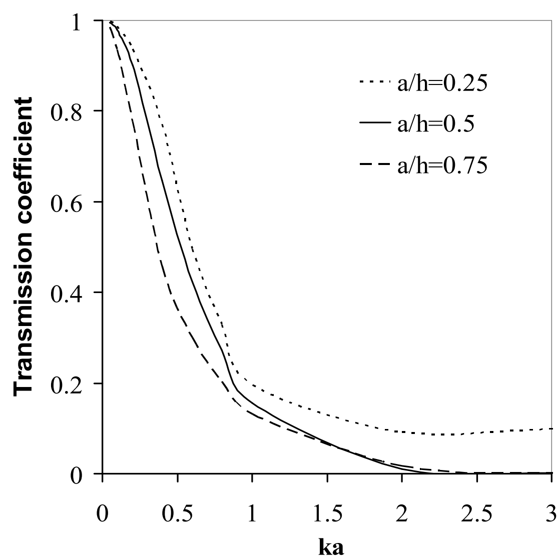

Figure 13. Modelled transmission coefficients for wave transmission past a cylindrical floating structure of infinite extent.

Floating Dock of Square Planform

Yue et al. (1976) have presented complete solutions of the full 3-d Laplace equation for wave scattering by a floating dock of square planform situated in water of constant depth (Figure 14). Note that this is not an x-z problem anymore and the TL-approximations cannot be used with the 1-dimensional equation (17). Instead, they are used with two-dimensional equation (1), to which Bessel-Fourier functions (e.g., Mei

1983, Xu et al. 1996) are applied as open ocean boundary conditions. Eq. (1) is then solved through the use of a finite-element grid developed with the graphical interface contained in the "Surface Water Modeling System" (Zundel et al. 1998). While developing the 2-d grid, the area covering the dock is also filled with finite elements; each node is assigned a depth equal to the local under-keel clearance times the correction factor α and q is set equal to zero. The parameters in the simulations are $a = h = 1$m, $d/h = 0.5$ and $ka = 1, 2, 3$ (corresponding to the cases described by Tsay and Liu (1983)). The results are shown in the form of amplification factors along the periphery of the dock in Figure 15. Although the correction factor α was developed in Chapter III using "infinitely long" floating structures, its use in the present multidirectional scattering problem produces results close to the full 3-d results for a wide range of *ka* values.

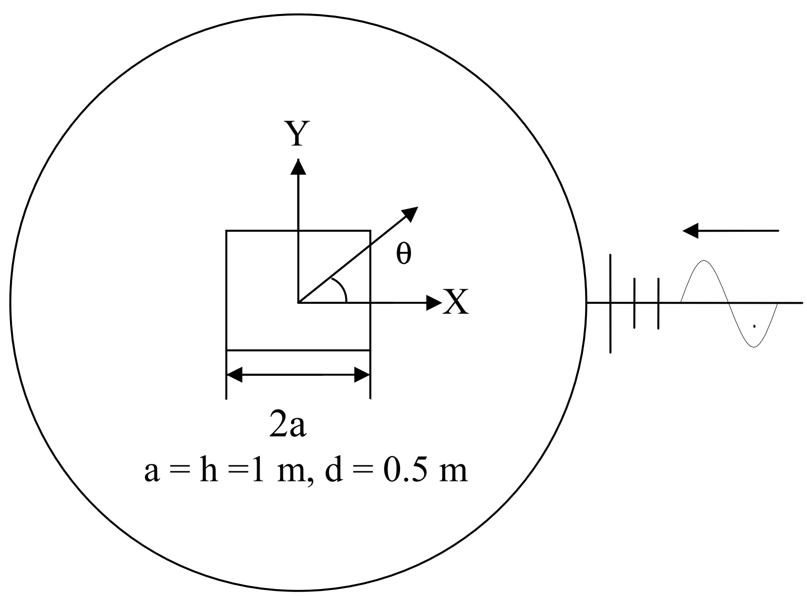

Figure 14. Wave propagation past a rectangular floating dock in circular domain of constant depth (x-axis corresponds to θ = 0).

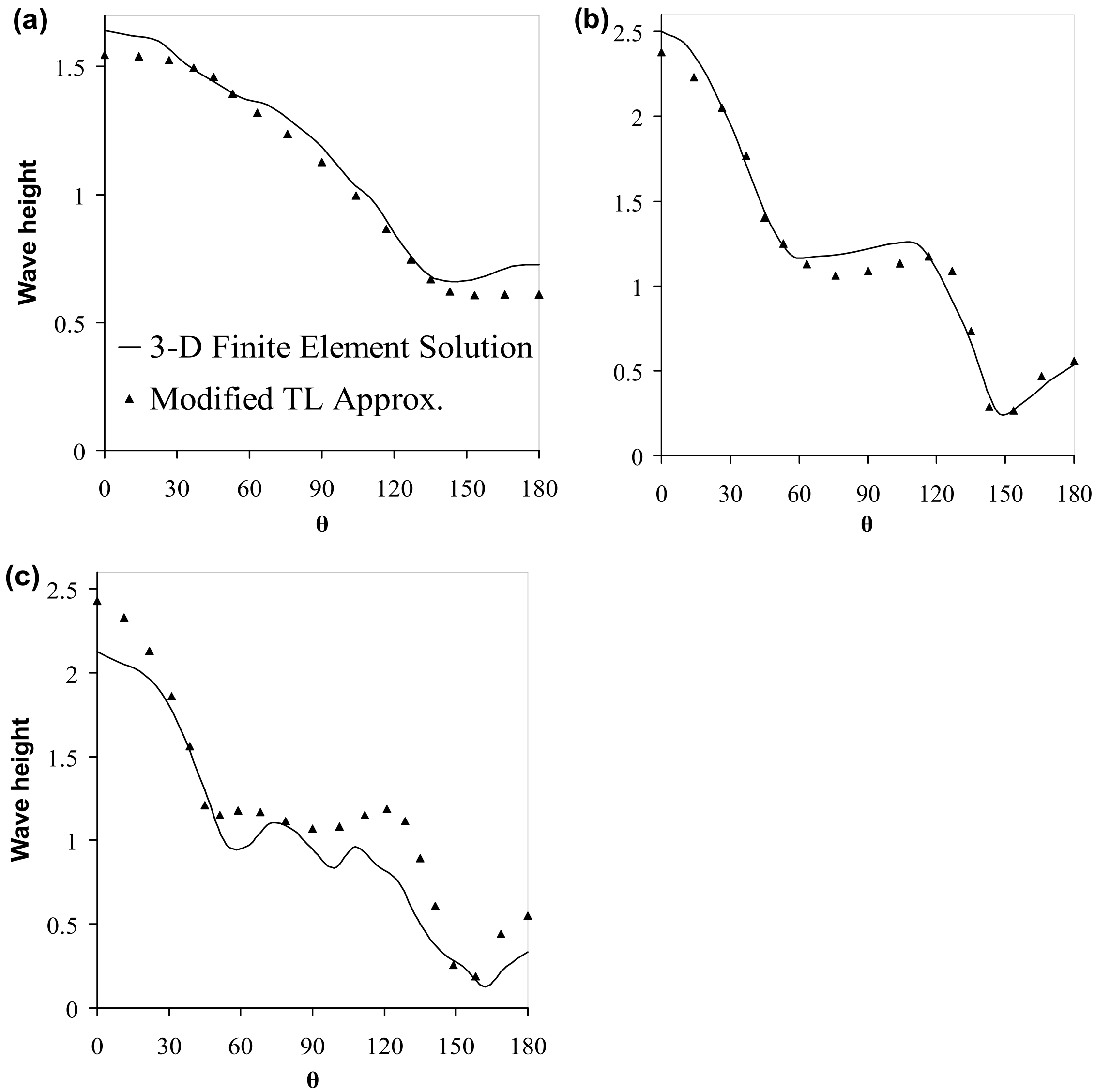

Figure 15. Wave height comparison. 3d solutions from Yue et al. (1976): (a) ka=1, (b) ka=2, (c) ka=3.

CHAPTER V

PRACTICAL APPLICATION

In view of the satisfactory results obtained with the modified TL approximation, it is used in conjunction with a frequently-used harbor wave modeling package called CGWAVE (e.g., Zubier et al. 2003; Demirbilek and Panchang 1998; Tang et al. 1999; Thompson et al. 2002) to demonstrate the effect of floating docks in a marina. This work was primarily done by Li et al. (2005), on the basis of correction factors (α) determined earlier in the thesis. Most of this harbor modeling was done as an expansion of a project done by Mr. Li and Professor Panchang. All this description is taken from Li et al. (2005).

The application pertains to ongoing design studies for the expansion of Douglas Harbor, situated on the west side of the Gastineau Channel in Alaska. The channel is approximately 2 km wide, and one angle of wave incidence that is of interest to design considerations is normal incidence across the channel.

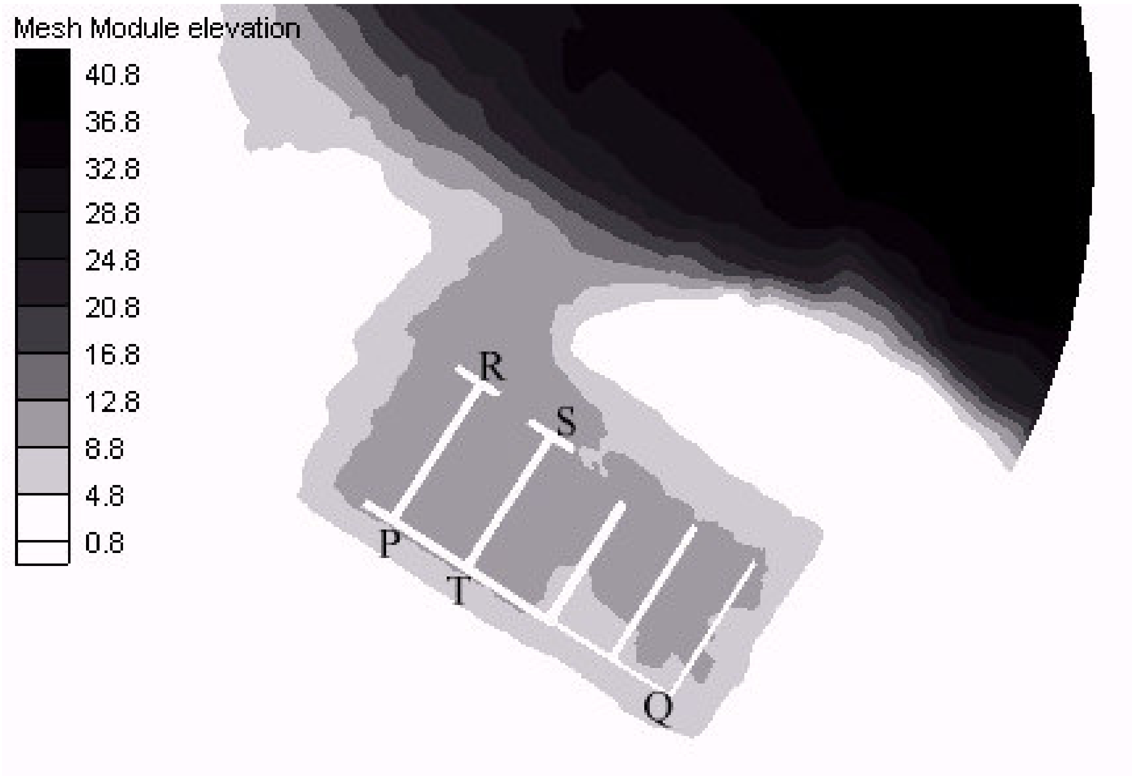

Figure 16. Bathymetry for **a** portion of Douglas Harbor modeling domain containing 5 floating docks, depth in meters.

The depth in the harbor, which is approximately 325 m by 165 m in size, varies from approximately 9.5 m to very small values at the coastal boundary. (The location of this boundary fluctuates due to a high tidal regime; only one tidal condition is described here). A part of the bathymetry is shown in Figure 16. For discussion purposes we consider linear wave conditions with input period = 4.4 s and height = 2 m, although design wind wave conditions at the site may be different. A triangular finite-element grid with 14 points per wavelength was constructed; this resulted in approximately 180,000 nodes and 355,000 elements. The coastal boundary was assigned zero reflection. The open boundary, denoted by the semicircle in Figures 17 and 18, was treated as per the mathematical formulation developed by Panchang et al. (2000). A depth-limited breaking criterion was applied to the solution of eq. [1], although other breaking models could also be used (Zhao et al. 2001).

The results in Figure 17, depicting modeled phases and wave heights for the case with no docks, show penetration of waves into the harbor and a nearly classical diffraction effect. The maximum wave height near the harbor entrance (near A) is approximately 2.6 m representing an amplification of 1.3. However, the uniform phase pattern in the harbor is considerably distorted when 5 docks (of widths varying between 1.8 m and 4.8 m) are inserted in the domain. (The docks are assumed to be fixed and the wave field is assumed to be unaffected by the tethering mechanisms.) The simulation with the docks is accomplished by simply highlighting the grids representing the dock and modifying the depth (using the appropriate correction factor α to change the under-keel depth d_1 to αd_1); also, the grid resolution in the vicinity of the docks must be increased because the water depths are now smaller. This is not difficult to implement since most grid generators allow "automatic refinement" in selected areas. The resulting simulation (Figure 18) shows three differences with Figure 17. First, the presence of the docks leads to considerable attenuation of the waves on the lee side of the dock marked PQ in Figure 16. Second, reflections within the dock area, manifested by the distorted phase pattern and considerable wave height variability are seen in the model results. For example, the waves are as high as 3.2 m on the up-wave side of the dock PQ (near P); also, changes in the range of 2.6 m to 0.2 m in the region between RP and ST occur. This suggests that proper attention must be paid to the appropriate location of the docks to avoid undesirable motion of docked boats. Finally, and perhaps most significantly, a reflective pattern (near B), created largely by the dock RP, propagates up-wave from the docks into the area outside the harbor. As a result, considerably larger wave heights occur near the harbor entrance (indicated by darker patterns in the gray-scale plots); the maximum value is approximately 3.9 m (near B), representing (nearly) standing waves and an increase of almost 50% relative to the case without the docks. This increase is consistent with the amplification on the upstream side seen in the theoretical results in Figure 15. The standing wave pattern in the entrance channel area may be of some concern from a navigation perspective, especially for small craft utilizing such harbors. At this time the U.S. Army Corps of Engineers (Alaska District Office) is in the process of designing a re-configured entrance channel at Douglas Harbor that includes a new wave barrier on the north side and an extension of the existing breakwater on the south side (not shown).

It is noted that these results are shown only by way of demonstration of the use of the modified TL-approximation; the effect of mechanisms not included here such as frictional damping and wave-wave interaction (e.g., Panchang & Demirbilek 2001) may lead to different solutions.

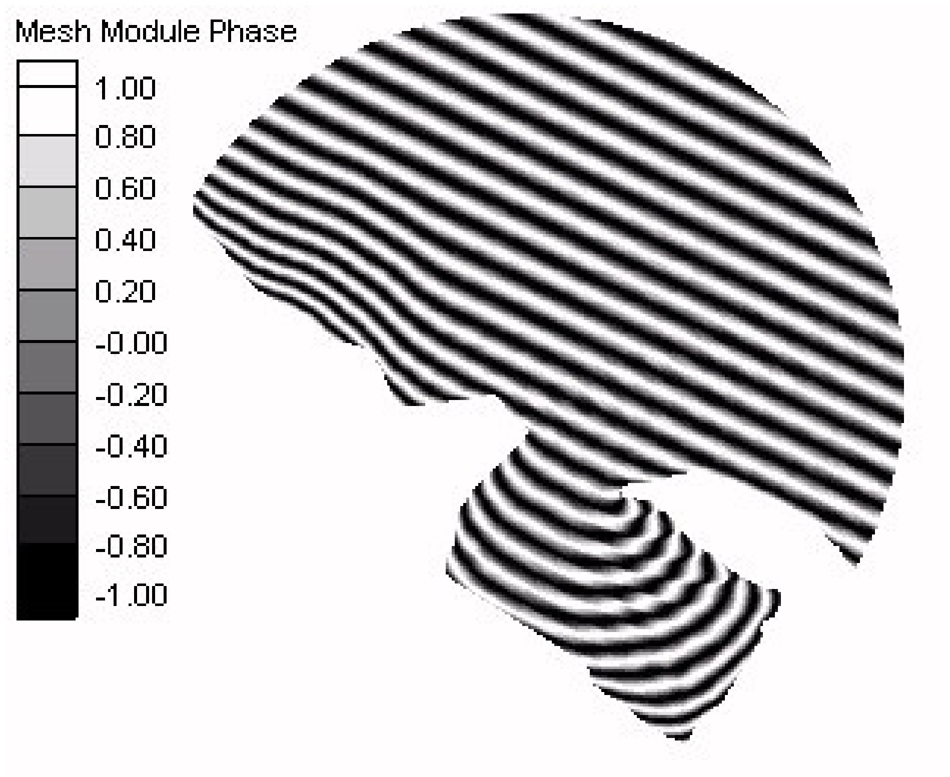

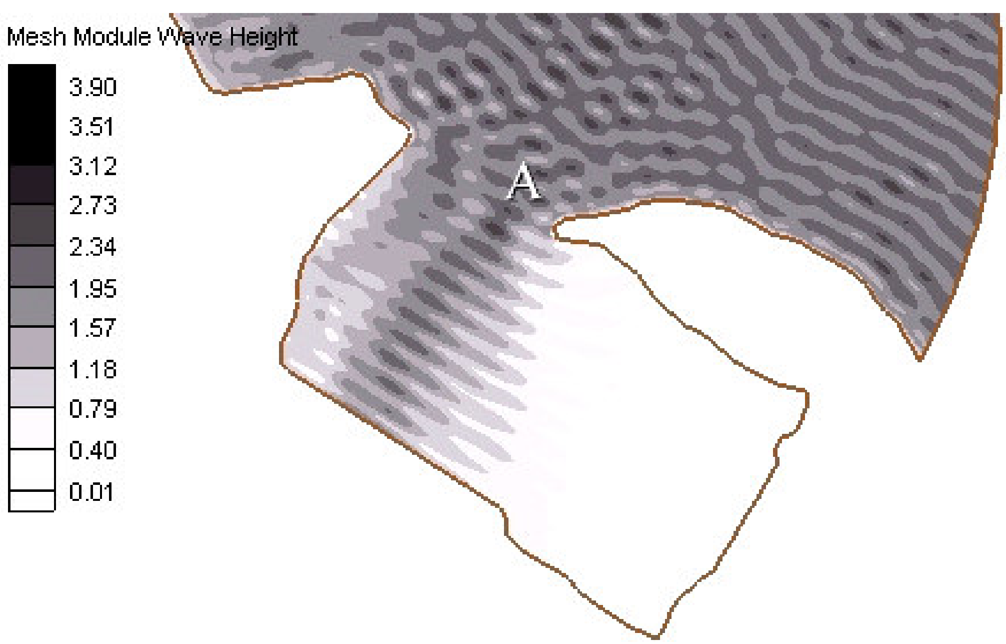

Figure 17. Modelled phases and wave heights (m) in Douglas Harbor, with no docks.

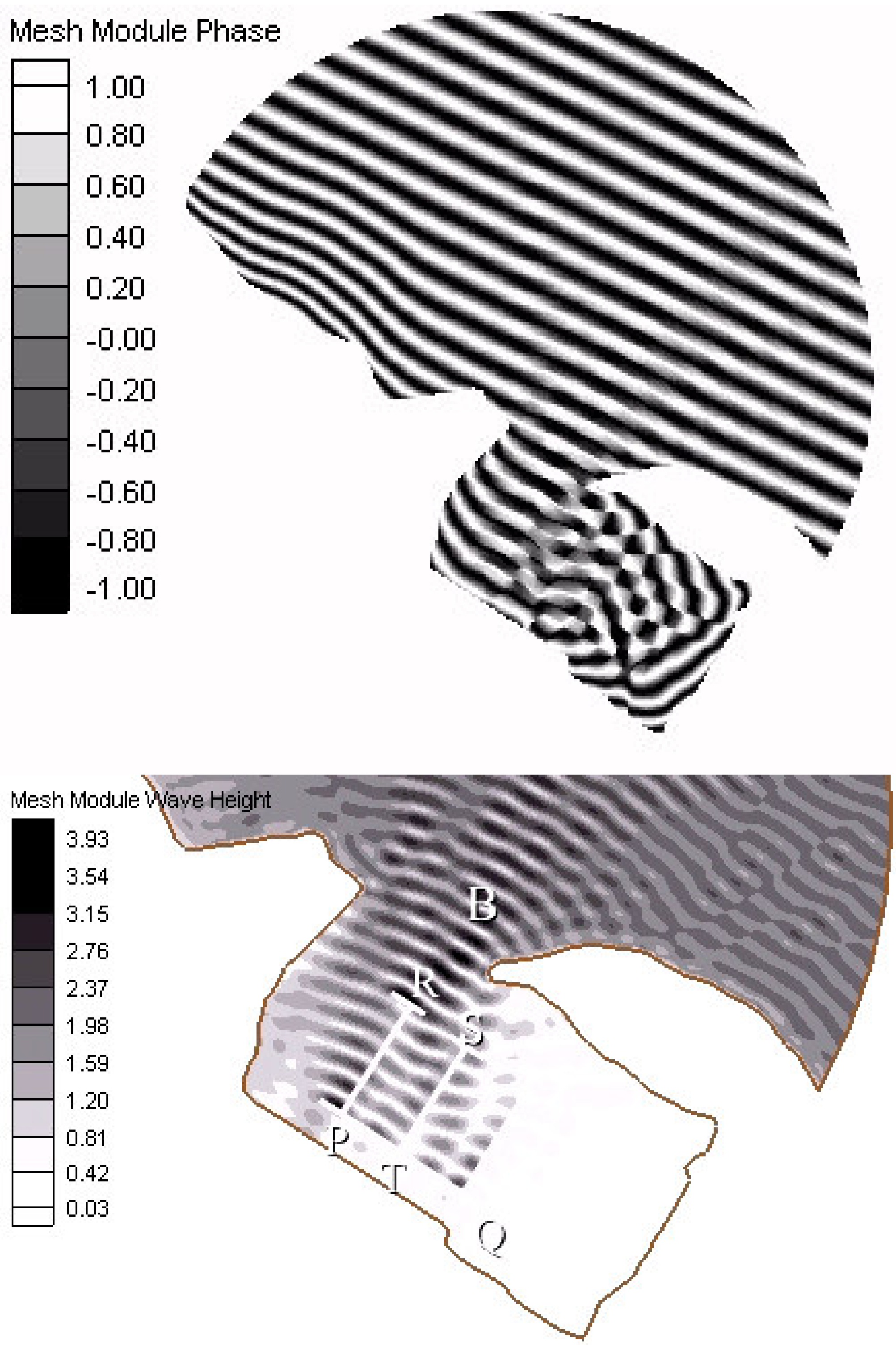

Figure 18. Modelled phases and wave heights (m) in Douglas Harbor, with docks.

CHAPTER VI

SUMMARY AND CONCLUSIONS

The approximate method proposed by Tsay and Liu (1983) to incorporate floating structures in a two-dimensional elliptic harbor wave model is extremely convenient for the engineers to implement with currently available harbor wave modeling technology; however, it produces results which deviate considerably from the solution of the Laplace equation. By performing a large number of tests that compared solutions of the TL-approximation with those of the Laplace equation, a simple modification to the original TL-approximation was developed. This involves adjusting the under-keel depth by a factor $\alpha = A ln(ka)+B$, where A and B are given in Figure 8 for different values of relative submergence. The modified TL-approximation yields improved results over the original TL-approximation, when compared to both laboratory data and theoretical results, for a wide range of conditions. By way of practical demonstration, the modified TL-approximation is applied to Douglas Harbor (Alaska). For the case examined, the floating docks in the harbor are shown to considerably attenuate the wave heights near some of the harbor coastlines relative to currently-used models (that do not contain the facility to model the effects of the floating structures). However, the docks are shown to create a reflective pattern in the dock area and another reflective pattern that propagates up into the area of the harbor entrance/navigation channels; these reflections, in principle, can be detrimental to transiting or docked vessels unless the dock layout is properly designed.

In the future, field validation of the model enhancement described here will be performed. Many basic harbor wave simulation models have been validated in the field (e.g., Panchang and Demirbilek 2001), but without the effects of docks. The performance of the model under the influence of irregular waves will also be examined.

REFERENCES

Booij, N., Ris, R. C., Holthuijsen, L.H., 1999. A third-generation wave model for coastal regions. 1. Model description and validation. Journal of Geophysical Research 104(c4), 7649-7666.

Bova, S. W., Breshears, C. P., Cuicchi, C., Demirbilek, Z., Gabb, H. A., 2000. Dual-level parallel analysis of harbor wave response using MPI and OpenMPI. International Journal of High Performance Computing Applications 14(1), 49-64.

Chamberlain, P. G., Porter, D., 1995. The modified mild-slope equation. The Journal of Fluid Mechanics 291,393-407.

Demirbilek, Z., Panchang, V. G., 1998. CGWAVE: a coastal surface water wave model of the mild slope equation. TR CHL-98-26, USACOE R&D Center, Vicksburg, MS.

Drimer, N., Agnon, Y., Stiassnie, M., 1992. A simplified analytical model for a floating breakwater in water of finite depth. Applied Ocean Research 14, 33-37.

Ijima, T., Chou, C. R., Yoshida, A., 1976. Method of analysis for two-dimensional water waves problems. Proc. Int. Con. on Coastal Engineering, Honolulu, HI, pp. 2717-2736.

Kostense, J. K., Dingemans, M. W., van den Bosch, P., 1988. Wave-current interaction in harbours. Proc. 21st Int. Conf. Coastal Engineering, ASCE, New York, pp. 32-46.

Koutandos, E. V., Karanbas, Th. V., and Koutitas, C. G., 2004. Floating breakwater response to waves action using Boussinesq model coupled with a 2DV elliptic solver. Journal of Waterway, Port, Coastal and Ocean Engineering 130(5), 243-255.

Madsen, P.A., Sorensen, O. R., 1992. A new form of the Boussinesq equations with improved linear dispersion characteristic. Part 2: a slowly-varying bathymetry. Coastal Engineering 18, 183-205.

Martin, P.A., Dixon, A.G., 1983. The scattering of regular surface waves by a fixed, half-immersed, circular cylinder. Applied Ocean Research 5(1), 13-23.

Mattioli, F., 1996. Dynamic response of the lido channel to wave motion in the presence of movable barriers. Il Nuovo Cimento 19(1), 177-194.

Mei, C. C., 1983. The Applied Dynamics of Ocean Surface Waves. John Wiley, New York.

Ohyama, T, Tsuchida, M., 1997. Expanded mild-slope equations for the analysis of wave-induced ship motion in a harbor. Coastal Engineering 30(1-2), 359-373.

Panchang, V. G., Ge, W., Cushman-Roisin, B., Pearce, B. R., 1991. Solution to the mild-slope wave problem by iteration. Applied Ocean Research 13(4), 187-199.

Panchang, V. G., Chen, W., Xu, B., Schlenker, K., Demirbilek, Z., Okihiro, M., 2000. Effects of exterior bathymetry in elliptic harbor wave models, Journal of Waterway, Port, Coastal & Ocean Engineering 126(2), 71-78.

Panchang, V. G., Demirbilek, Z., 2001. Simulation of waves in harbors using two-fimensional elliptic equation models". In: Liu, P. (Ed.), Advances in Coastal & Ocean Engineering. World Scientific, Singapore, pp. 125-162.

Panchang, V. G., 2005. A modeling strategy for incorporating the effect of floating structures on waves in a coastal region. Report submitted to the Office of Naval Research, Arlington, VA.

Ris, R. C., Holthuijsen, L.H., Booij, N., 1999. A third-generation wave model for coastal regions. 2. Verification. Journal of Geophysical Research 104(c4),7667-7681.

Tang, Y., Ouellet, Y., Ropars, Y., 1999. Finite element modelling of wave conditions inside Sainte-Therese-de-Gaspe harbour, Quebec. Proc. Canadian Coastal Conference, Fraser Delta, pp. 737-748.

Sarpkaya, T., Isaacson, M., 1981. Mechanics of Wave Forces on Offshore Structures. Van Nostrand Reinhold, New York.

Thompson, E. F., Demirbilek, Z., 2002. Wave climate and wave response, 2025 plan, Kahului Harbor, Hawaii. USACOE, ERDC, TR-02-21, Vicksburg, MS.

Thompson E. F., Bottin, R. R., Shak, A. T., 2002. Monitoring of entrance channel navigation improvements at Morro Bay Harbor, Morro Bay, California. USACOE, ERDC, TR-02-18, Vicksburg, MS.

Tsay, T.-K., Liu, P.L.-F., 1983. A finite element model for wave refraction and diffraction. Applied Ocean Research 5(1), 30-37.

Wei, G., Kirby, J.T., Grilli, S. T., Subramanya, R., 1995. A fully nonlinear Bossinesq model for surface waves. 1. Highly nonlinear unsteady waves. The Journal of Fluid Mechanics 205, 397-419.

Xu, B., Panchang, V. G., Demirbilek, Z., 1996. Exterior reflections in elliptic harbor wave models. Journal of Waterway, Port, Coastal and Ocean Engineering 122(3), 118-126.

Yue, K. P., Chen, H. S., Mei, C. C., 1976. A hybrid element method for calculating three-dimensional water wave scattering, TR No. 215, Ralph M. Parsons Laboratory, Department of Civil Engineering, MIT, Cambridge, MA.

Zhao, L., Panchang, V. G., Chen, W., Demirbilek, Z., Chhabbra, N., 2001. Simulation of breaking effects in a two-dimensional harbor wave prediction model. Coastal Engineering 42(4), 359-373.

Zubier, K., Panchang, V. G., Demirbilek, Z., 2003. Simulation of waves at Duck (North Carolina) using two numerical models. Coastal Engineering Journal 45(3), 439-470.

Zundel, A. K., Fugal, A. L., Jones, N. L., Demirbilek, Z., 1998. Automatic definition of two-dimensional coastal finite element domains. Proc. 3rd Int. Conf. Hydroinformatics. Ed. V. Babovic and L. C. Larsen. A. A. Balkema, Rotterdam, pp. 693-700.

VITA

Zhaoxiang Tang was born on April 4, 1976 in Zigong City, Sichuan Province, China. He got his Bachelor of Engineering degree in Naval Architecture in 1999 from Harbin Engineering University (HEU). He worked in Shanghai Merchant Ship Design and Research Institute as a naval architect from 1999-2002. He came to Texas A&M University (TAMU) in 2003 to pursue his Master of Science degree in ocean engineering in the Department of Civil Engineering. His future plan after getting his M.S. degree is to continue his graduate study towards the degree of Doctor of Philosophy and then pursue challenging research or technical work in the field of ocean engineering.

His permanent address is South Apartment 209 No.3 Tower, Hongcaonan Road, Shanghai 20023, China. His email address is tangzhaoxiang@hotmail.com and Johnson.tang2004@gmail.com.